Original Article

COX-2-related tumor immune microenvironment in non-small cell lung cancer: a novel signature to predict hot and cold tumor

Tiangong Wang[1], Ying Luo[1,2], Qi Zhang[1], Yanping Shen[1], Min Peng[1], Ping Huang[1,2], Zijian Zhou[1,2], Xinyi Wu[1,2], Ke Chen[1]

[1]Department of Radiochemotherapy, The Affiliated People's Hospital of Ningbo University, Ningbo, China; [2]Medical School of Ningbo University, Ningbo, China

Contributions: (I) Conception and design: T Wang, K Chen; (II) Administrative support: K Chen; (III) Provision of study materials or patients: Q Zhang, Z Zhou; (IV) Collection and assembly of data: T Wang, Y Luo; (V) Data analysis and interpretation: T Wang; (VI) Manuscript writing: All authors; (VII) Final approval of manuscript: All authors.

Correspondence to: Ke Chen. Department of Radiochemotherapy, The Affiliated People's Hospital of Ningbo University, Ningbo, China. Email: qizheng0704@sina.com.

Background: At present, non-small cell lung cancer (NSCLC) remains a great threat to the health of people worldwide. Immune checkpoint inhibitors (ICIs) have shown positive results in the treatment of advanced NSCLC. However, the treatment response of ICIs is not stable and unpredictable. We used a bioinformatics analysis to determine a novel signature to diagnose the hot and cold tumor in NSCLC which may guide the programmed cell death protein 1/programmed cell death 1 ligand 1 (*PD-1/PD-L1*) therapeutic strategy.

Methods: The RNA-seq dataset and clinical data of 485 lung adenocarcinoma (LUAD) and 473 lung squamous cell carcinoma (LUSC) samples from The Cancer Genome Atlas (TCGA) database. Tumor infiltrating immune cells was calculated by CIBERSORT algorithm and ConsensusClusterPlus was used to classify the hot and cold tumor. Least absolute shrinkage and selection operator (LASSO) regression, Support Vector Machine (SVM) and Gaussian Mixture Model (GMM) were performed to determine the diagnostic area under curve (AUC) of novel signature of ICIs treatment. Overall survival (OS) analysis was based on the Kaplan-Meier statistical method.

Results: In this study, we found that the expression of *PD-1/PD-L1* is associated with *COX2* (*PTGS2*) expression. We identified novel signatures [*STMN3*, *KIRREL1*, *SH2D3C*, *VCL*, *PDCD1*, *CD274*, *PTGS2*, combined diagnostic (AUC) =0.838], in order to diagnose the hot and cold tumor subtype to indicate the treatment response of *PD-1/PD-L1* inhibitor in NSCLC. Furthermore, we found that in hot tumor subtype, high *PDCD1* expression group had worse OS than low *PDCD1* expression group (P=0.047); high *SH2D3C* expression group had worse OS than low SH2D3C expression group either (P=0.003). *SH2D3C* was correlated to *PD-1* expression in NSCLC samples (R=0.49, P<0.001). We speculated that *SH2D3C* likely plays a crucial role in *PD-1*-related immunotherapy in NSCLC patients. Pathway enrichment showed that the focal adhesion (P=0.005) and actin cytoskeleton (P=0.022) pathways were associated with OS.

Conclusions: This study aimed to identify the classification of hot and cold tumors, and develop a novel signature to predict the ICI treatments response for *PD-1/PD-L1* high expression NSCLC patients.

Keywords: Non-small cell lung cancer (NSCLC); immunotherapy response subtypes; diagnostic signatures; tumor immune microenvironment (TIME)

Submitted Jan 27, 2022. Accepted for publication Mar 18, 2022.
doi: 10.21037/jtd-22-257
View this article at: https://dx.doi.org/10.21037/jtd-22-257

Introduction

Lung cancer remains the leading cause of malignant tumor mortality worldwide (1). Non-small cell lung cancer (NSCLC) accounts for approximately 85% of all lung cancer cases, and is divided into three types: adenocarcinoma, squamous cell carcinoma, and large cell carcinoma (2), of which adenocarcinoma and squamous cell carcinoma are the most prevalent. Despite the continuous improvement in the tertiary prevention of lung cancer, the 5-year overall survival (OS) for NSCLC is still not ideal, especially for patients with late stage disease (less than 10%) (3). With the support of next-generation sequencing technology, some of molecular subtypes have been classified, facilitating the progress of clinical application of targeted therapy and immunotherapy.

Immunotherapy is a method of immune system activation to fight and efficiently remove tumor cells (4). Immune checkpoint inhibitors (ICIs) are most important immunotherapeutic modalities, and have offered a novel path for the treatment of NSCLC. ICIs are already being applied in first-line NSCLC therapy, and are generally combined with chemotherapy and radiotherapy (3). The most popular ICIs are a series of programmed cell death protein 1/programmed cell death 1 ligand 1 (*PD-1/PD-L1*) inhibitors, which block the *PD-1/PD-L1* pathway between tumor cells and T cells, and activate infiltrating T cells to attack tumor cells (5). However, not all NSCLC patients benefit from ICIs treatment. Despite the fact that several ICI therapy-related clinical studies have found that patients with high *PD-1* expression can benefit from ICI treatment, some patients with high *PD-1* expression still do not benefit from *PD-1* inhibitors. T cell exhaustion may be the important reason. When CD8+ T cell is under the condition of exhaustion, even with positive *PD-1* expression, it does not have ability to eliminate the tumor cells (6). Likewise, it is found that *PD-L1* is translated inside the nuclear having a new function to promote the tumorigenesis but not binding on the surface of cellular membrane (7). It explains that a part of patients have high *PD-1/PD-L1* expression but have little response to the *PD-1/PD-L1* inhibitor.

The tumor microenvironment (TME) is an internal environment where tumor cells reside; it is extremely complex and contains various tumor-related and immune cells, which constitute the entire microenvironment in tumor tissue, and involves interaction between different cell types (8). However, the mechanism underlying the low response to ICI treatment remains unclear. The TME in different NSCLC patients is not identical, which may explain patients undergoing ICI treatment have diverse therapeutic outcomes. Additionally, the tumor immune microenvironment (TIME) is correlated with tumor immunotherapy. Various immune cells in the TME are not identical, which suggests that the response to ICI treatment is also correlated to the TIME.

Cyclooxygenase-2 (*COX-2*) is associated with inflammation-related diseases, such as cancer. *COX-2* is secreted by cancer-associated fibroblasts (CAFs), macrophage type 2 cells, and cancer cells in the TME, and have the ability to promote an inflammatory response in the local environment and induce tumor progression, metastasis, and drug resistance (9). *COX-2* inhibitors have long been used for pain and to reduce inflammation, but evidence regarding the effectiveness of *COX-2* inhibitors in anti-tumor therapy has emerged (10). However, in TME the mechanism of *COX-2* influencing the *PD-1/PD-L1* therapy is unclear. It is necessary to dig out the relationship between *COX-2* and TME to help us deeply understand how *COX-2* play a biological role in TME.

In this study, we relied on the RNA-seq data and used bioinformatics analysis to find out a novel diagnostic signature of hot and cold tumor and a potential gene target may have relations between each subtype. We integrated lung adenocarcinoma (LUAD) and lung squamous cell carcinoma (LUSC) RNA sequencing (RNA-seq) dataset from The Cancer Genome Atlas (TCGA) database as the NSCLC dataset. Tumor infiltrating immune cells were calculated through the CIBERSORT algorithm and the result was classified by the machine learning method to distinguish the hot and cold tumor subtypes which have different response to ICIs therapy. Additionally, we categorized the subtypes into hot and cold tumor groups, and performed an in-depth analysis the different genes between these two types to screen for novel diagnostic signatures of ICI therapy and mine hub genes for further study. We present the following article in accordance with the TRIPOD reporting checklist (available at https://jtd.amegroups.com/article/view/10.21037/jtd-22-257/rc).

Methods

In this study, we collected the LUAD and LUSC RNA-seq and clinical data from TCGA database. CIBERSORT algorithm used to estimate the immune cell infiltration, then we used infiltration data to classified the hot and cold

tumor subtypes. Weighted correlation network analysis (WGCNA) was used to recognize the genes related to the hot and cold tumor. LASSO, SVM and GMM statistic methods were used to calculate the hot and cold tumor diagnostic signature. Kaplan-Meier analysis, GO and KEGG enrichment were used to compute the hot and cold tumor OS and potential pathway. The study was conducted in accordance with the Declaration of Helsinki (as revised in 2013).

Data collection and treatment

The RNA-seq dataset and clinical data of 485 LUAD and 473 LUSC samples from TCGA database were downloaded from University of California-Santa Cruz (UCSC) Xena website (URL: https://xena.ucsc.edu/). The LUAD and LUSC datasets were combined into NSCLC data, samples without clinical data matched were excluded. Gene expression in the RNA-seq matrix was transformed into Transcripts per million (TPM) from count. The approximate number of tumor infiltrating immune cells was calculated by CIBERSORT algorithm (R script v1.03, Aaron M. Newman, Stanford University). The script and signature matrix file, LM22, was downloaded from the CIBERSORT website (URL: http://CIBERSORT.stanford.edu/). The RNA-seq matrix input was changed to log2(TPM+1). Following calculation by CIBERSORT, each sample was found to have infiltration level of 22 types of immune cells. A method of unsupervised machine learning, R package ConsensusClusterPlus, was utilized to classify the subtypes from all samples in the NSCLC data. The ConsensusClusterPlus was employed based on the following conditions: maxK =20, reps =20, pItem =0.8, and pFeature =1.

Features extraction for predicting the tumor immune subtype

WGCNA was performed using the WGCNA package to analyze the correlation between hub gene modules and clinical features. The Glmnet package (Jerome Friedman, Trevor Hastie, Robert Tibshirani) was used for least absolute shrinkage and selection operator (LASSO) regression analysis of the variable selection and regularization, in order to screen for predictors in the gene expression matrix. Supervised machine learning was used to identify the genes diagnosis the hot or cold tumor, which was computed by Support Vector Machine (SVM) algorithm. Package of e1071 (David Meyer, Evgenia Dimitriadou, Kurt Hornik, Andreas Weingessel and Friedrich Leisch, TU Wien) and msvmRFE.r program (John Colby) were applied to realize the SVM algorithm. To find the predicted signatures of the tumor immune subtypes, the Gaussian Mixture Model (GMM) was used to calculate the best performing group of genes, after screening by the SVM.

Drug response

To identify the potential anti-tumor drugs in hot and cold tumors, the signature genes were applied to the Genomics of Drug Sensitivity in Cancer (GDSC) database, to compare the areas under the curve (AUCs) of drug response clusters in hot and cold tumors.

Pathway enrichment

The Database for Annotation, Visualization, and Integrated Discovery (DAVID) v6.8 (URL: https://david.ncifcrf.gov/) was applied to enrich the Kyoto Encyclopedia of Genes and Genomes (KEGG) and Gene Ontology (GO) hub gene-related pathways. Program R (R Foundation for Statistical Computing, Vienna, Austria) was used to organize the enrichment result from DAVID and draw the diagrams. Gene Set Variation Analysis (GSVA) was used to estimate the gene set enrichment variation and calculate the relationship between pathways.

Statistical analyses and diagram plots

The Kruskal-Wallis test was used to compare the gene expression between each group of samples. The AUC was used to calculate the predictable score for binary data, the acceptable AUC threshold values is 0.5. The Spearman test was applied to estimate the correlation coefficients between genes or pathways. OS analysis was based on the Kaplan-Meier (KM) statistical method. $P<0.05$ was considered to indicate a statistically significant difference. All the plots were draw by ggplot package (H. Wickham, Springer-Verlag, New York, USA). All of statistical analyses and plots were based on Program R (V4.03 and V4.10).

Results

TIME in NSCLC

The RNA-seq data of NSCLC, including 485 LUAD and 473 LUSC from TCGA database. NSCLC RNA-seq matrix was used to calculate the composition of 22 types

of immune cells in each sample through CIBERSORT algorithm (*Figure 1A,1B*). Based on the infiltration of 22 types of immune cells, the NSCLC samples were clustered via consensus clustering, which is a method of unsupervised machine learning. According to the cumulative distribution functions (CDF) and area under the CDF curve, when K=6, the area of both of two plots reached an approximate maximum (*Figure 1C,1D*). Then we check the cluster assignment of columns, cluster in K=6 was indicative of unstable membership (*Figure 1E*). It suggests that when parameter K=6, consensus and cluster are confidence. The consensus matrix, which was comprised of six clusters, was extracted for further analysis (*Figure 1F*).

COX-2 associated with hot and cold tumor

According to the infiltration of cluster of differentiation 8 positive ($CD8^+$) T cells and the expression of *PD-1/PD-L1* in these six clusters, three ICI-related subtypes of NSCLC were identified (*Figure 2A-2C*). Also, three immunophenotypes were observed as immune-inflamed, immune-excluded, and immune deserted, respectively, based on the spatial quantification of $CD8^+$ T cells in the tumor tissue (11). Cluster 2 had high-level infiltration of $CD8^+$ T cells and high *PD-1/PD-L1* expression, and was classified as an immune-inflamed type. Clusters 1 and 6 with medium infiltration of $CD8^+$ T cells, but low *PD-1/PD-L1* expression, were classified as immune-excluded types. The remaining clusters, which exhibited low-level infiltration of $CD8^+$ T cells and low *PD-1/PD-L1* expression, were classified as the immune desert type. Pre-clinical evidence has suggested that *COX-2* inhibitors combining with ICIs can promote anti-tumor T-cell activation (12). Prostaglandin-endoperoxide synthase 2 (*PTGS2*, aliases of *COX-2*) expression is lower in the immune-inflamed type than in the other types, whereas *PTGS2* expression is non-differentiated in the other two types (*Figure 2D*). It has been reported that overexpression of the *COX-2* gene inhibits dendritic cell maturation, resulting lower anti-tumor $CD8^+$ T cell infiltration. The results of our study are highly consistent with previous research. The Kaplan-Meier OS between three the immune subtypes (immune-desert type median OS =44.8 months, immune-exclude type median OS =57.5 months, immune-inflamed type median OS =66.1 months) in NSCLC were not significantly different (log rank P=0.1, two tailed test) (*Figure 2E*), which could be due to the fact that the TCGA clinical data does not include the ICI intervention history.

Hub genes identified through WGCNA

Based on the aforementioned result, we decided to combine the immune-excluded type and the immune desert type as cold tumors, and defined the immune-inflamed type as a hot tumor. Compared to hot tumors, the response rate of patients with cold tumors is relatively low (13). To determine the differential gene profiles between cold and hot tumors, WGCNA was employed to assess the gene expression profiles of both types. Firstly, we cleaned the data by excluding outlier samples (*Figure 3A*). In the network topology analysis, we selected the power 3 for soft-thresholding, which produced an output of 20 modules of different genes after network analysis (*Figure 3B,3C*). In 20 modules, consider the correlation coefficient of cold tumor (R=0.2, P<0.001), hot tumor (R=–0.2, P<0.001) and *COX-2* expression (R=0.26, P<0.001), the greenyellow module is most relevant to the clinical traits (*Figure 3D*). In the greenyellow module, 924 genes were chosen for subsequent analysis.

Screen hub genes and explore novel signatures

LASSO regression was used to screen the module genes from the WGCNA analysis to remove the multi-collinearity genes. We set the parameter as lambda.min =0.011, and 116 genes were then filtered from the 924 genes (*Figure 4A,4B*). Supervised machine learning SVM was applied to classify the relationship between hot and cold tumor classification in these 116 genes, and 10 genes were found to exhibit the minimum cross validation error. (*Figure 4C*). Each gene was scored by the SVM algorithm, and we selected the top 10 related genes (*XIRP1*, *CLMP*, *TNFSF4*, *STMN3*, *KIRREL1*, *SH2D3C*, *MFAP2*, *C1S19*, *PLVAP*, and *VCL*) to combine with the three core genes (*PDCD1*, *CD274*, and *PTGS2*) for further analysis. GMM was applied to count the AUC values of 8,191 groups consisting of 13 potential genes. The purple group, which included seven genes (*STMN3*, *KIRREL1*, *SH2D3C*, *VCL*, *PDCD1*, *CD274*, *PTGS2*), had the highest diagnostic AUC value (*Figure 4D*). These seven genes consisted of a combined diagnostic signature with an AUC of 0.838, which was considerably higher than that of any single gene alone (*Figure 4E*), suggesting that this new diagnostic signature could be a predictor of the therapeutic effect of ICIs.

SH2D3C is a potential target and related to the OS of hot tumor

Kaplan-Meier survival analysis shows that the OS of

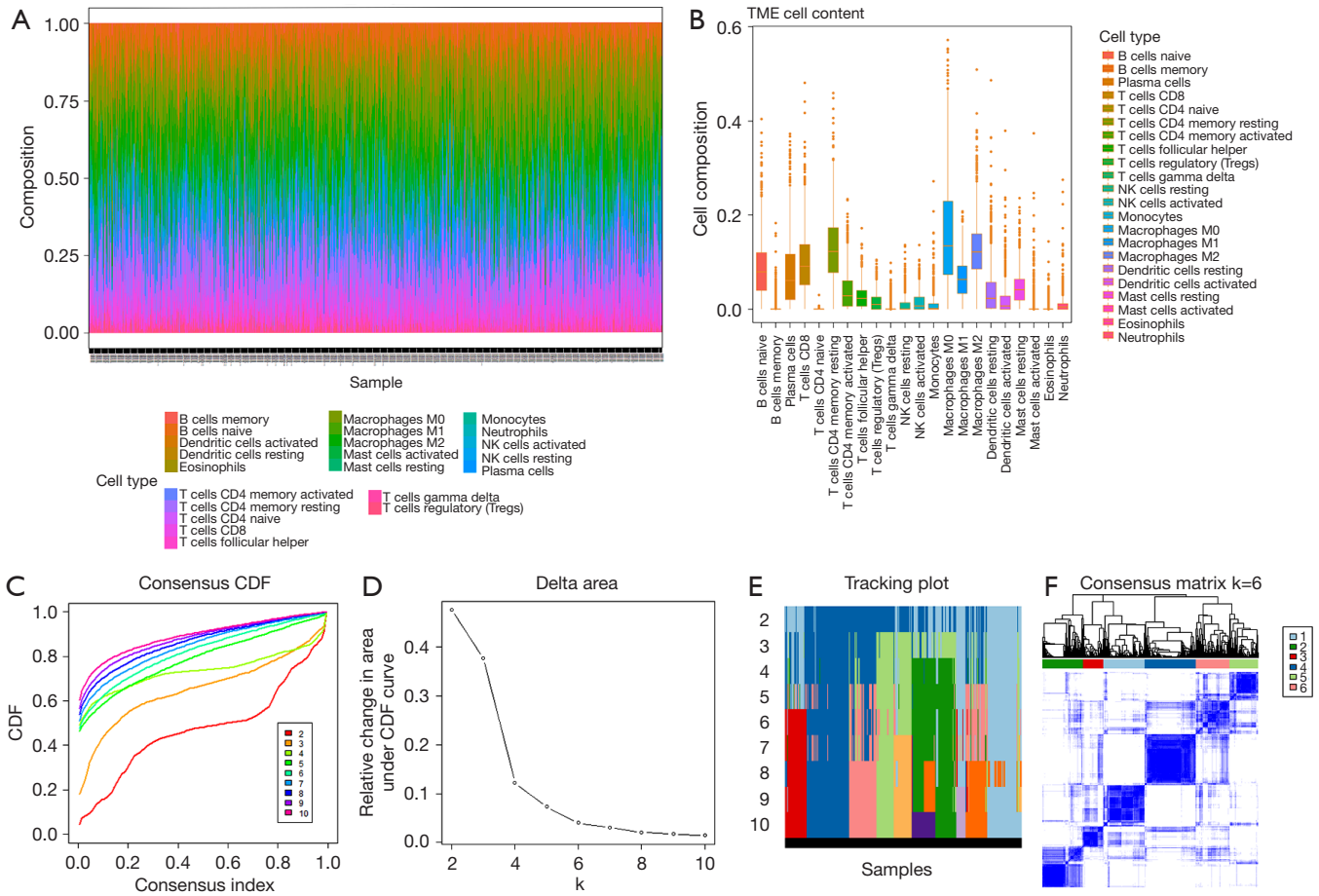

Figure 1 TIME in NSCLC. (A,B) The composition of immune cells in NSCLC samples was evaluated by CIBERSORT. (C) CDF of cluster result. (D) Delta area of cluster result. (E) Tracking plot of cluster result (y-axis means K=2–10). (F) The consensus cluster matrix. TIME, tumor immune microenvironment; CIBERSORT, an algorithm to estimate the immune cell composition from gene expression of samples; NK cells, natural killer cells; TME, tumor microenvironment; CDF, cumulative distribution functions; NSCLC, non-small cell lung cancer.

PDCD1 in NSCLC was not significant (log rank P=0.76, two tailed test); the OS of *SH2D3C* in NSCLC was not significant (log rank P=0.45, two tailed test). In hot tumor, high *PDCD1* expression group had worse OS than low *PDCD1* expression group (log rank P=0.047, two tailed test); high *SH2D3C* expression group had worse OS than low SH2D3C expression group either (log rank P=0.003, two tailed test). In cold tumor, the OS of *PDCD1* (log rank P=0.49, two tailed test) and *SH2D3C* (log rank P=0.36, two tailed test) was not significant. It suggested that the OS of *PDCD1* and *SH2D3C* was not associated with that of the NSCLC patients (*Figure 5A,5B*) or the cold tumor subtype (*Figure 5C,5D*). Meanwhile, OS was significantly related to the hot tumor subtype (*Figure 5E,5F*). These findings revealed that *PDCD1* and *SH2D3C* could be survival-relevant biomarkers; however, the remaining genes were not. *SH2D3C* expression was moderate relative to *PDCD1* expression (R=0.49, P<0.001), which suggests that *SH2D3C* is an important gene may interact with *PD-1* to influence TME and ICI treatment in NSCLC (*Figure 5G*). To understand which drug is suitable for both hot and cold tumors, we searched more than 300 compounds in the GDSC database. By comparing the tumor gene expression profiles and NSCLC cell expression matrix of hot tumor and cold tumors, we found that the AUC of methotrexate (*Figure 5H*) was lower in hot tumors (P=0.0023) than cold tumor, and that the AUC of trichostatin-A (*Figure 5I*) was lower in cold tumors (P=0.023). This signifies that

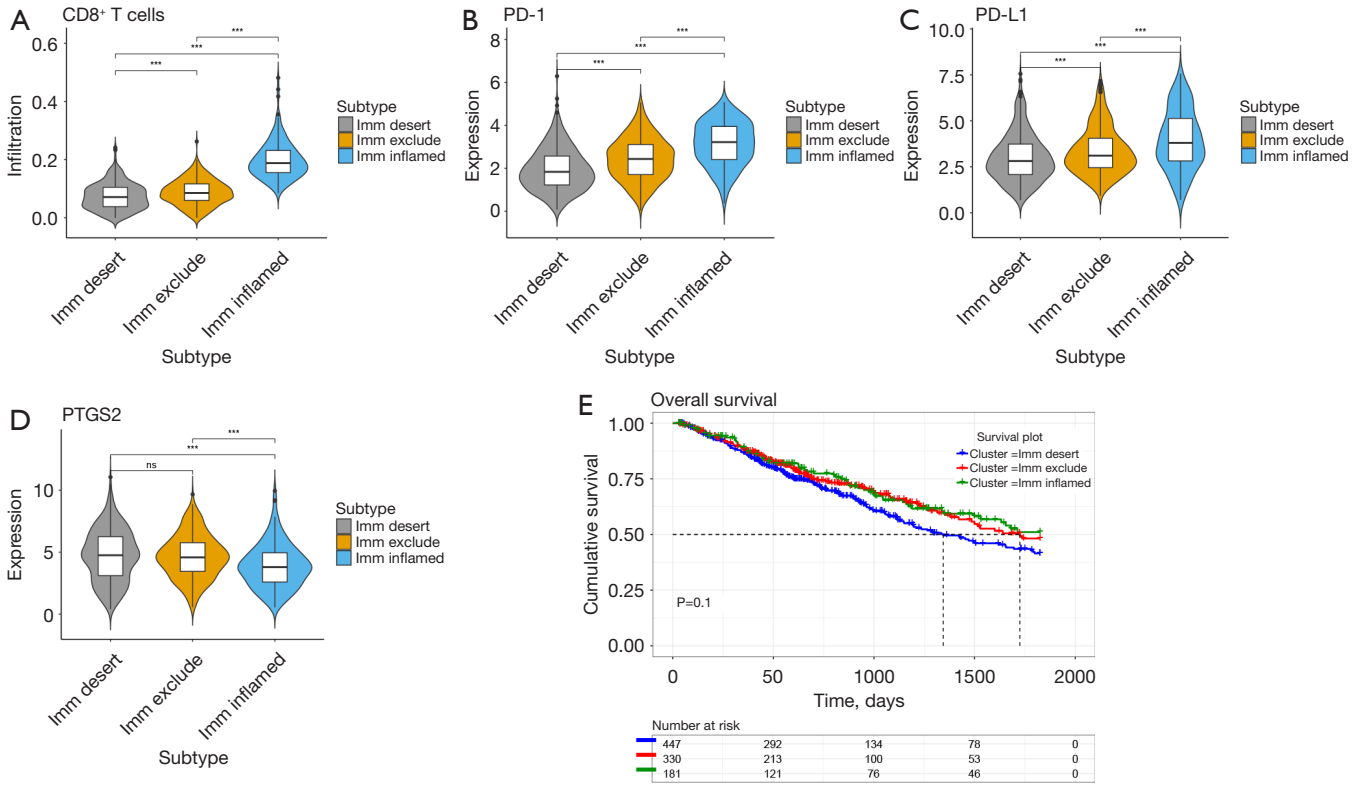

Figure 2 *COX-2* associated with hot and cold tumor. (A) Infiltration level of CD8+ T cells in the three subtypes of NSCLC. (B-D) Gene expressions of *PD-1*, *PD-L1*, and *PTGS2* in the three subtypes of NSCLC. (E) 5-year overall survival of the three subtypes of NSCLC. The Kruskal-Wallis test was used to compare each subtype, ***, P<0.001; ns, P>0.05. Kaplan-Meier was used to analyze overall survival. NSCLC, non-small cell lung cancer; *PD-1*, programmed cell death protein 1; *PD-L1*, programmed cell death 1 ligand 1.

methotrexate is effective hot tumors and trichostatin-A could be administered to cold tumor patients.

Pathway enrichment related to hot and cold tumor

After WGCNA analysis, we acquired 924 genes to have next step analysis to explore the GO and KEGG pathway enrichment related to the phenotype between hot and cold tumor. The enriched pathways from the DAVID database (*Figure 6A*,*6B*) were analyzed using GSVA to further calculate the relationship between these pathways (*Figure 6C*). We found that the mechanism of focal adhesion and actin cytoskeleton pathways maybe play a crucial role between hot and cold tumor. Survival analysis showed that high enrichment group of the focal adhesion pathway had significantly worse OS than low enrichment group (log rank P=0.005, two tailed test), and high enrichment group of the actin cytoskeleton pathway had worse OS than low enrichment group too (log rank P=0.022, two tailed test) (*Figure 6D*,*6E*).

Discussion

ICI therapy has changed the treatment landscape of multiple advanced cancers, including NSCLC (13). In fact, ICI treatment is the first choice of many late stage patients. It is generally acknowledged that NSCLC patients have high *PD-1/PD-L1* expression, and thus could have a significant response to *PD-1/PD-L1* inhibitor treatment. Nevertheless, a proportion of *PD-1/PD-L1*-positive patients has little or no response to ICI therapy. Recently, clinicians have tended to use *PD-1/PD-L1* DNA expression, tumor mutation burden (TMB), and microsatellite instability/mismatch repair-deficient (MSI/dMMR) to predict the therapeutic effect of ICIs (14). As with the TMB, MSI/dMMR-positive patients still have a certain probability of no response to ICI treatment, with even some patients even experiencing hyper-progressive disease after treatment.

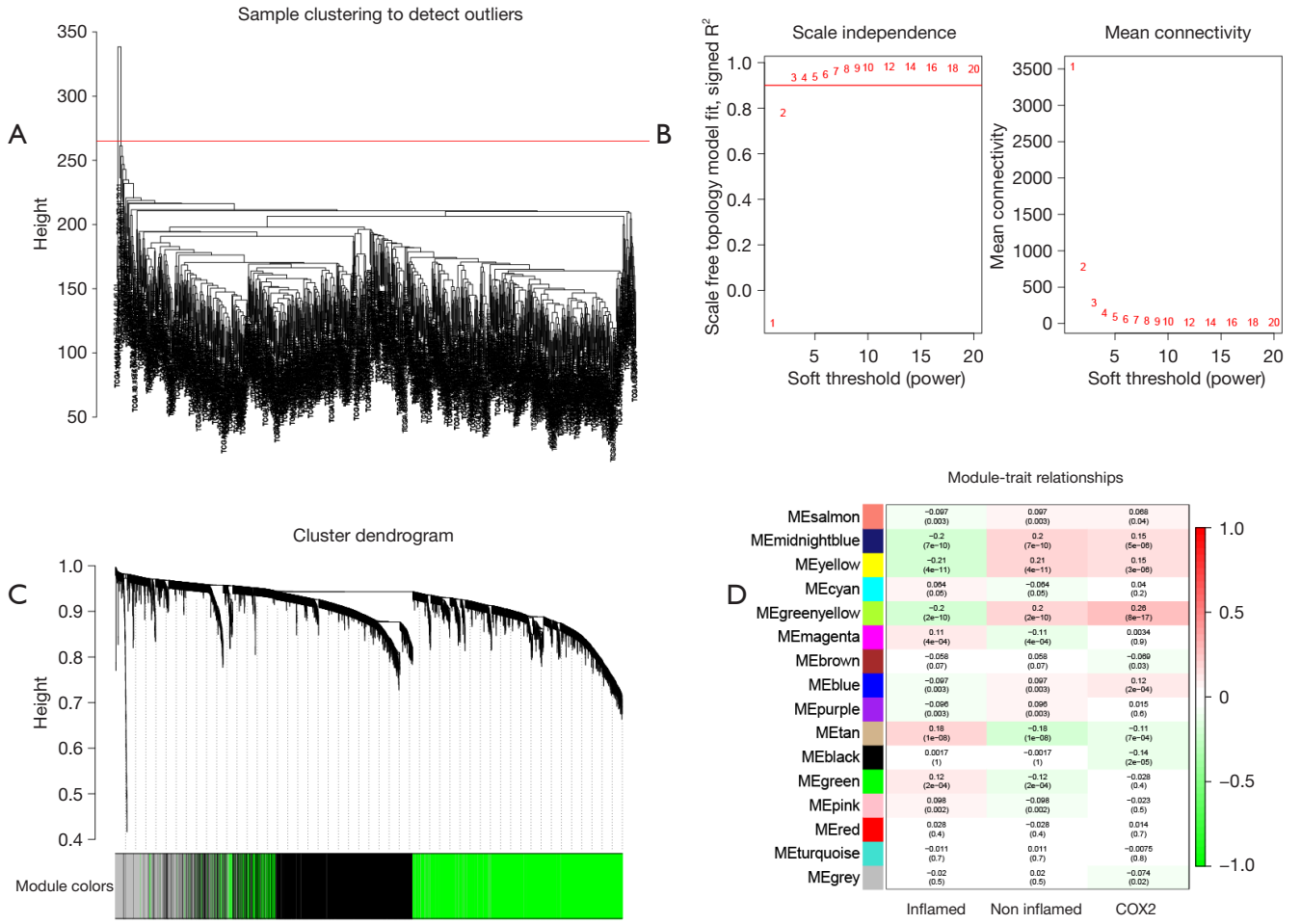

Figure 3 Hub genes identified through WGCNA. (A) The red line excludes the outlier samples. (B) The red line is the 90% level of scale independence; we selected the soft threshold power of 3. (C) The cluster dendrogram of the modules. (D) The relationship between the module and clinical traits (the number of bar chart –1 to 1 is the correlation index). WGCNA, weighted correlation network analysis.

The TME refers to the area in which tumor cells reside, and contains support cells such as blood vessels, CAFs, extracellular matrix, immune-associated cells, and various of signal molecules secreted by different kinds of cell in the TME (15). The TME does not only include substrates; some life activities, such as hypoxia, oxidative stress, metabolic alterations, also occur in the TME (16). All of these processes interact with each other; otherwise, the content change will influence the immune profile of the TME. Considering of TME heterogeneity, even both with high expression of PD-1, the response of ICIs treatment still has huge gap between the patients. There must be some other factors regulating the TME that respond to ICI drugs.

Classifying tumors as either hot or cold is the basic way of distinguishing tumors that could respond to ICI therapy from those that will not. Infiltration of $CD8^+$ T cells into the tumor is most important factor to identify hot and cold tumors. In our study, we found that a cluster identified by unsupervised machine learning, which showed high-level $CD8^+$ T cell infiltration, was correlated to *PD-1/PD-L1* expression and was classified as a hot tumor subtype (11). In other clusters, CD8+ T cells and *PD-1/PD-L1* were relatively lower than those of the hot tumor cluster, and were thus defined as cold tumors. To understand the difference between the hot and cold tumors, investigated the different genes of these two subtypes, hoping to identify some new biomarkers to predict the response to ICI therapy prior to treatment.

COX-2 is a famous molecule that correlated to

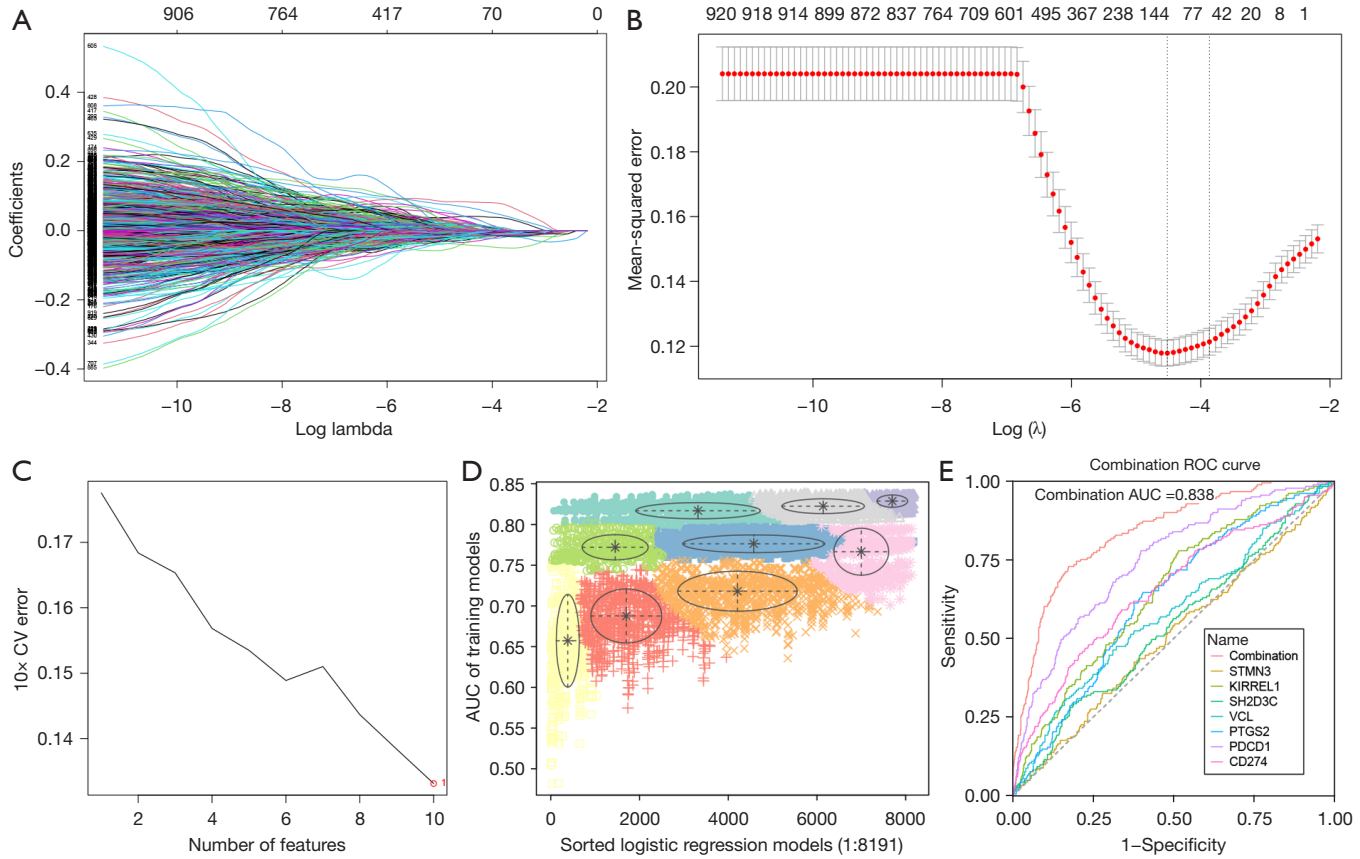

Figure 4 Screen hub genes and explore novel signatures. (A) Coefficients of each sample of the LASSO regression model. (B) The mean-squared error of the LASSO regression model result. (C) Plot of generalization error. When top features input is 10 the SVM result has the lowest CV error. (D) The GMM model was used to screen the best AUC performance group of signatures to judge cold and hot tumors. (E) The combination AUC value of 7 genes is 0.838, it is higher than each of gene. LASSO, least absolute shrinkage and selection operator; CV, cross-validation; SVM, Support Vector Machine; GMM, Gaussian Mixture Model; AUC, area under the curve; ROC, receiver operating characteristic.

inflammation (17). *COX-2* inhibitors are common drugs applied in many chronic inflammatory diseases. Chronic inflammation over a prolonged period is a crucial factor in tumorigenesis. *COX-2* is also strongly correlated to the TME, and some important cells the TME (such as CAFs, macrophage type 2 cells, and tumor cells) can secrete the *COX-2*. Thus, dysregulated control of the TME can induce *COX-2* overexpression (9,18,19). In our analysis, we found that *COX-2* expression was lower in hot tumors than in cold tumors. However, in cold tumors, *COX-2* expression in immune-excluded and immune desert subtypes were not different, and the infiltration of $CD8^+$ T cells in these two types was significantly different. This result is consistent with previous research. In the TME, cells can act to both promote and inhibit the inflammatory effect, and the balance of these opposing actions in infiltrating cells is likely the key reason why some patients, who have the same high expression of *PD-1/PD-L1*, have totally different ICI treatment responses (20). Meanwhile, previous research has indicated that *COX-2* inhibitors have the potential value to be anti-tumor assistant drugs and improve the therapeutic outcomes of patients (15). However, these drugs are not strongly recommended for use as a first-line clinical treatment by officials. Considering the availability of these medicines, we believe that *COX-2* inhibitor still presents a potential complementary treatment for tumor immunotherapy.

However, the mechanism through which *COX-2* inhibitors change the TME and induce anti-tumor effects is still unclear. In our study, we aimed to employ

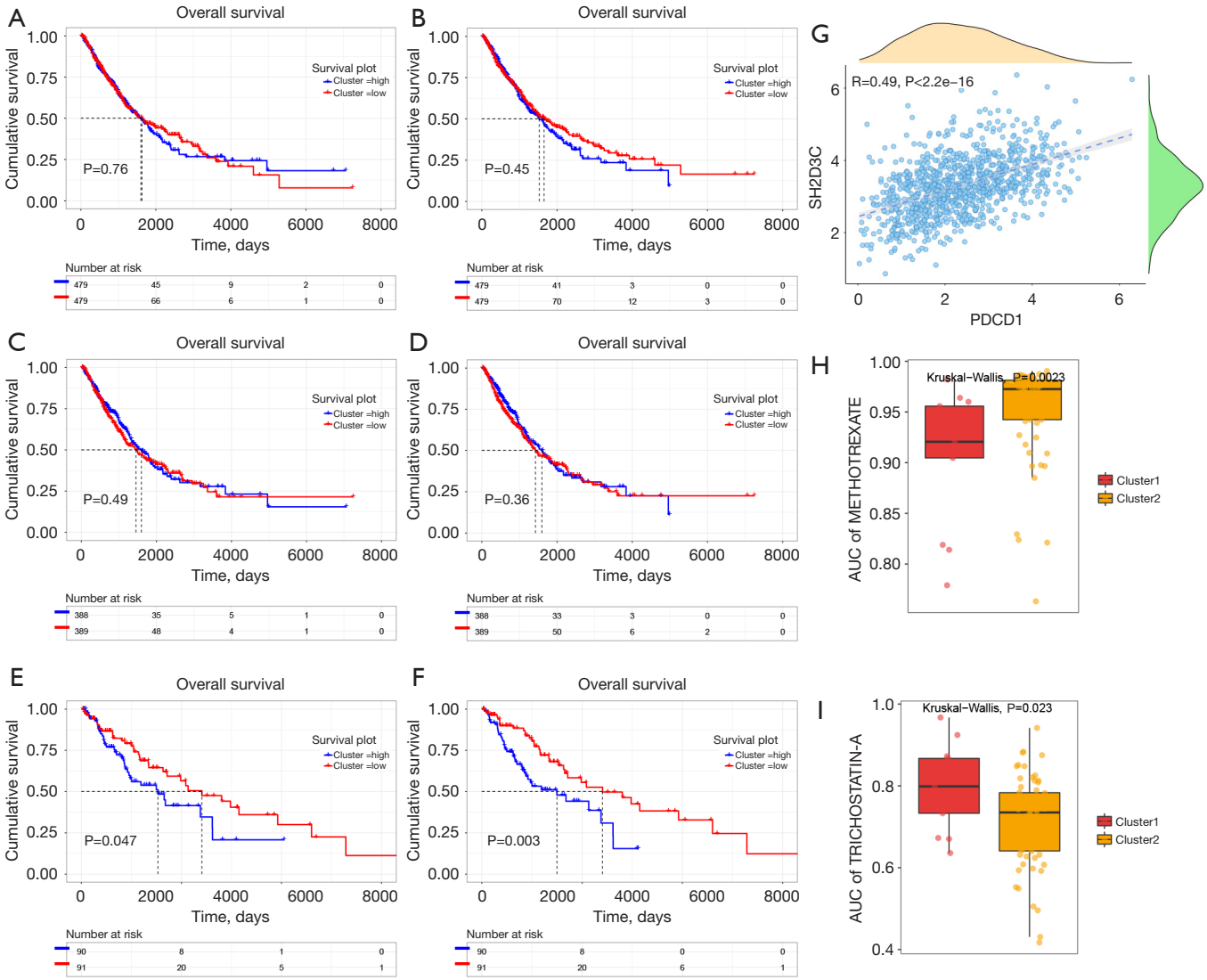

Figure 5 *SH2D3C* is a potential target and related to the OS of hot tumor. (A) OS of *PDCD1* in all NSCLC samples. (B) OS of *SH2D3C* in all NSCLC samples. (C) OS of *PDCD1* in NSCLC cold tumor type samples. (D) OS of *SH2D3C* in NSCLC cold tumor type samples. (E) OS of *PDCD1* in NSCLC hot (immune-inflamed) tumor type samples. (F) OS of *SH2D3C* in NSCLC hot (immune-inflamed) tumor type samples. (G) Correlation between *PDCD1* and *SH2D3C* in NSCLC data. (H,I) Potential anti-tumor drugs in cold and hot tumors were analyzed using GDSC database. OS, overall survival; NSCLC, non-small cell lung cancer; GDSC, Genomics of Drug Sensitivity in Cancer. AUC, area under curve.

bioinformatics analysis to investigate big data related to NSCLC to screen the crucial genes of immunotherapy response prediction. We defined the hot and cold tumor subtypes of NSCLC data by infiltration of $CD8^+$ T cells, *PD-1/PD-L1* expression, and *COX-2* gene expression. Using a series of analyses, we established a predictable signature that included seven hub genes to predict whether a tumor was hot or cold before treatment. Our signature had an AUC value of 0.838, which is a delightful discovery. However, due to limitations of the available sources, we did not validate this result. In future research, we plan to collect the tumor tissue or blood samples of patients before administration of ICI therapy explore the predictive value of the signature in the real world.

In this study, we also found an important gene, known as *SH2D3C*, which had a good correlation with *PD-1*

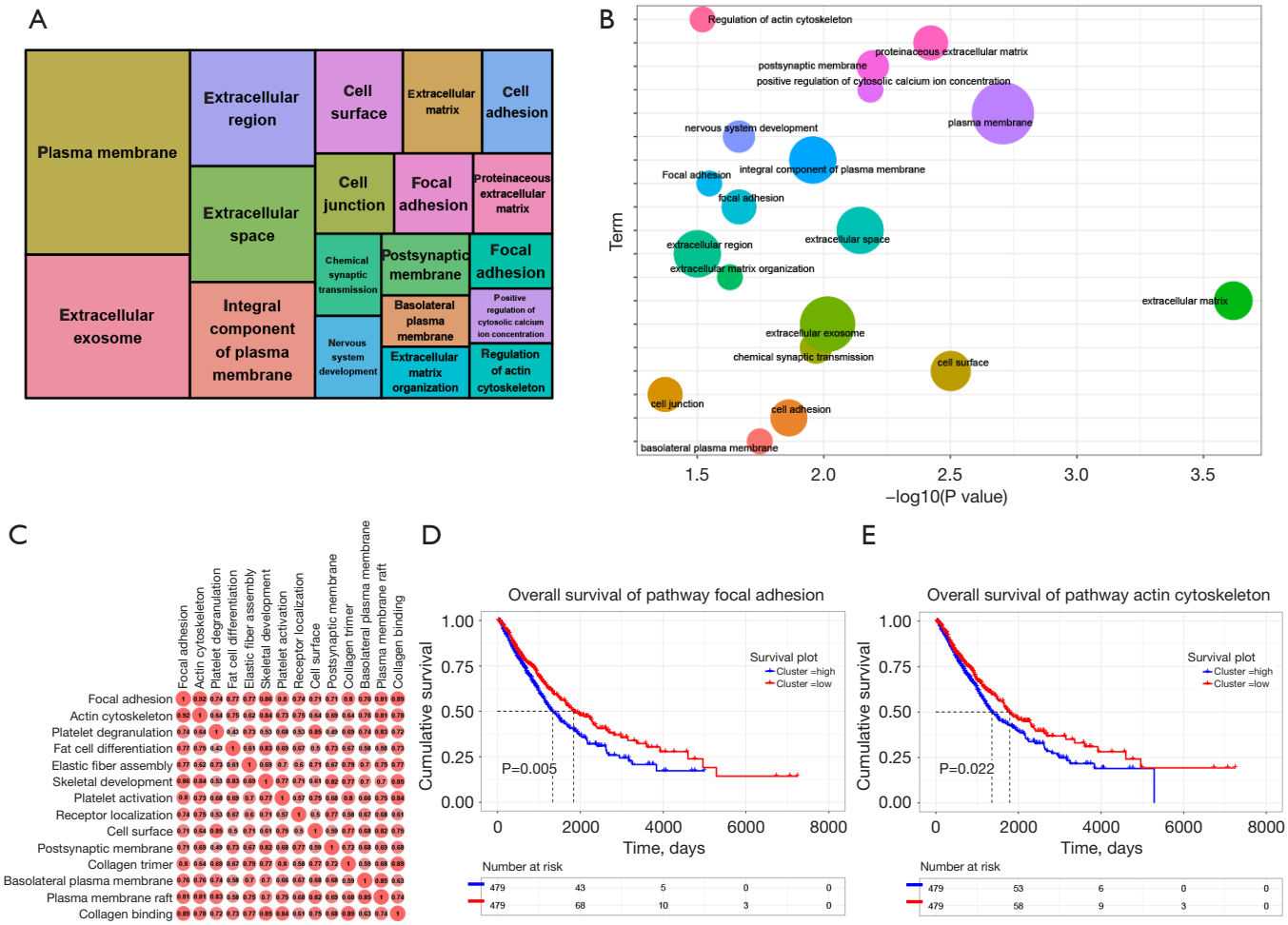

Figure 6 Pathway enrichment related to hot and cold tumor. (A,B) Significant pathway enrichment using the DAVID database. (C) Correlation between the significant pathways was calculated by GSVA. (D,E) Overall survival of the focal adhesion and actin cytoskeleton pathways in all NSCLC samples. DAVID, Database for Annotation, Visualization, and Integrated Discovery; GSVA, Gene Set Variation Analysis; NSCLC, non-small cell lung cancer.

expression. Furthermore, NSCLC patient with high expression of *SH2D3C* and *PD-1* may benefit to the OS in hot tumor type. We speculated that *SH2D3C* may play an important role the *PD-1*-related tumor immunotherapy. One previous study revealed that *SH2D3C* plays an oncological role in lung cancer and promotes tumor immune evasion by inhibiting and even excluding T cells in lung tumor environment (21). In further study, it is necessary to use the Clustered Regularly Interspaced Short Palindromic Repeats (CRISPR)-based method to screen the relative genes and downstream pathways. Regulating *SH2D3C* maybe help to discover novel immune-related pathways and understand the relationship between immunotherapy and the TME. *SH2D3C* may be a target that could change cold tumors into hot ones, and thus deserves further in-depth research.

Conclusions

In summary, the era of immunotherapy is still in the early days, and a large number of advanced NSCLC patients have already benefited from it. This paper aimed to utilize big data from the TCGA database to analyze the *COX-2*-related ICI treatment response signatures to predict cold and hot tumors, and improve the clinical treatment strategy. Additionally, *SH2D3C* is a potential treatment target for NSCLC. Immunotherapy combined with other treatments is being increasingly used as a first-line clinical treatment.

Through our study, we hope to identify some novel assistant medicines in immunotherapy, as well as a target that can reverse cold tumors into hot ones.

Acknowledgments

The authors would like to thank TCGA for sharing the LUAD and LUSC datasets.
Funding: This work was supported by the Ningbo Municipal Natural Science Foundation (No. 201401A6110062).

Footnote

Reporting Checklist: The authors have completed the TRIPOD reporting checklist. Available at https://jtd.amegroups.com/article/view/10.21037/jtd-22-257/rc

Conflicts of Interest: All authors have completed the ICMJE uniform disclosure form (available at https://jtd.amegroups.com/article/view/10.21037/jtd-22-257/coif). The authors have no conflicts of interest to declare.

Ethical Statement: The authors are accountable for all aspects of the work in ensuring that questions related to the accuracy or integrity of any part of the work are appropriately investigated and resolved. The study was conducted in accordance with the Declaration of Helsinki (as revised in 2013).

References

1. Sung H, Ferlay J, Siegel RL, et al. Global Cancer Statistics 2020: GLOBOCAN Estimates of Incidence and Mortality Worldwide for 36 Cancers in 185 Countries. CA Cancer J Clin 2021;71:209-49.
2. Travis WD, Brambilla E, Nicholson AG, et al. The 2015 World Health Organization Classification of Lung Tumors: Impact of Genetic, Clinical and Radiologic Advances Since the 2004 Classification. J Thorac Oncol 2015;10:1243-60.
3. Duma N, Santana-Davila R, Molina JR. Non-Small Cell Lung Cancer: Epidemiology, Screening, Diagnosis, and Treatment. Mayo Clin Proc 2019;94:1623-40.
4. McCune JS. Rapid Advances in Immunotherapy to Treat Cancer. Clin Pharmacol Ther 2018;103:540-4.
5. Efremova M, Rieder D, Klepsch V, et al. Targeting immune checkpoints potentiates immunoediting and changes the dynamics of tumor evolution. Nat Commun 2018;9:32.
6. Beltra JC, Manne S, Abdel-Hakeem MS, et al. Developmental Relationships of Four Exhausted CD8+ T Cell Subsets Reveals Underlying Transcriptional and Epigenetic Landscape Control Mechanisms. Immunity 2020;52:825-841.e8.
7. Du W, Zhu J, Zeng Y, et al. KPNB1-mediated nuclear translocation of PD-L1 promotes non-small cell lung cancer cell proliferation via the Gas6/MerTK signaling pathway. Cell Death Differ 2021;28:1284-300.
8. Junttila MR, de Sauvage FJ. Influence of tumour microenvironment heterogeneity on therapeutic response. Nature 2013;501:346-54.
9. Hashemi Goradel N, Najafi M, Salehi E, et al. Cyclooxygenase-2 in cancer: A review. J Cell Physiol 2019;234:5683-99.
10. Qiu HY, Wang PF, Li Z, et al. Synthesis of dihydropyrazole sulphonamide derivatives that act as anti-cancer agents through COX-2 inhibition. Pharmacol Res 2016;104:86-96.
11. Hegde PS, Chen DS. Top 10 Challenges in Cancer Immunotherapy. Immunity 2020;52:17-35.
12. Wang SJ, Khullar K, Kim S, et al. Effect of cyclo-oxygenase inhibitor use during checkpoint blockade immunotherapy in patients with metastatic melanoma and non-small cell lung cancer. J Immunother Cancer 2020;8:e000889.
13. Bonaventura P, Shekarian T, Alcazer V, et al. Cold Tumors: A Therapeutic Challenge for Immunotherapy. Front Immunol 2019;10:168.
14. Lizardo DY, Kuang C, Hao S, et al. Immunotherapy efficacy on mismatch repair-deficient colorectal cancer: From bench to bedside. Biochim Biophys Acta Rev Cancer 2020;1874:188447.
15. Hui L, Chen Y. Tumor microenvironment: Sanctuary of the devil. Cancer Lett 2015;368:7-13.
16. Augustin RC, Delgoffe GM, Najjar YG. Characteristics of the Tumor Microenvironment That Influence Immune

Cell Functions: Hypoxia, Oxidative Stress, Metabolic Alterations. Cancers (Basel) 2020;12:3802.
17. Yao C, Narumiya S. Prostaglandin-cytokine crosstalk in chronic inflammation. Br J Pharmacol 2019;176:337-54.
18. Ohtsuka J, Oshima H, Ezawa I, et al. Functional loss of p53 cooperates with the in vivo microenvironment to promote malignant progression of gastric cancers. Sci Rep 2018;8:2291.
19. Liu Y, Borchert GL, Surazynski A, et al. Proline oxidase, a p53-induced gene, targets COX-2/PGE2 signaling to induce apoptosis and inhibit tumor growth in colorectal cancers. Oncogene 2008;27:6729-37.
20. Pelly VS, Moeini A, Roelofsen LM, et al. Anti-Inflammatory Drugs Remodel the Tumor Immune Environment to Enhance Immune Checkpoint Blockade Efficacy. Cancer Discov 2021;11:2602-19.
21. Yeh YC, Lawal B, Hsiao M, et al. Identification of NSP3 (SH2D3C) as a Prognostic Biomarker of Tumor Progression and Immune Evasion for Lung Cancer and Evaluation of Organosulfur Compounds from Allium sativum L. as Therapeutic Candidates. Biomedicines 2021;9:1582.

Cite this article as: Wang T, Luo Y, Zhang Q, Shen Y, Peng M, Huang P, Zhou Z, Wu X, Chen K. *COX-2*-related tumor immune microenvironment in non-small cell lung cancer: a novel signature to predict hot and cold tumor. J Thorac Dis 2022;14(3):729-740. doi: 10.21037/jtd-22-257